

# Control of crystalline phase and morphology of calcium carbonate by electrolysis: Effects of current and temperature

著者	Miyazaki Toshiki, Arie Takashi, Shiroaki Yuki
journal or publication title	Ceramics International
volume	45
number	11
page range	14039-14044
year	2019-04-19
URL	<a href="http://hdl.handle.net/10228/00008196">http://hdl.handle.net/10228/00008196</a>

doi: <https://doi.org/10.1016/j.ceramint.2019.04.103>

Manuscript Number: CERI-D-18-09086R1

Title: Control of crystalline phase and morphology of calcium carbonate by electrolysis: effects of current and temperature

Article Type: Full length article

Keywords: Powders: chemical preparation; Biomedical applications; CaCO<sub>3</sub>

Corresponding Author: Dr. Toshiki Miyazaki,

Corresponding Author's Institution: Kyutech

First Author: Toshiki Miyazaki

Order of Authors: Toshiki Miyazaki; Takashi Aii; Yuki Shiroaki

Abstract: Calcium carbonate (CaCO<sub>3</sub>) can show various properties related to its different crystalline phases. For example, the aragonite phase has excellent mechanical strength, whereas the vaterite phase has high water solubility. Therefore, CaCO<sub>3</sub> is a useful material for various applications. Wet processes are known to be suitable for preparing metastable CaCO<sub>3</sub> polymorphs. Electrolysis has been proposed as a preparation method at ambient conditions. Although several electrolytic approaches have been reported, the effects of the applied current and temperature of the electrolyte on the crystalline phase and morphology of CaCO<sub>3</sub> remain unclear. In the present study, we attempted the electrochemical preparation of CaCO<sub>3</sub> particles with various electrolysis conditions and discuss the mechanism of CaCO<sub>3</sub> particle formation. The crystalline phase and morphology of the CaCO<sub>3</sub> precipitates markedly changed depending on the applied current and method of cooling the electrolyte. We assume that these factors were governed by the degree of change in temperature, supersaturation and pH of the electrolyte induced by differences in the electrolysis current.

1  
2  
3 **Control of crystalline phase and morphology of calcium carbonate by**  
4 **electrolysis: effects of current and temperature**  
5  
6

7 Toshiki Miyazaki<sup>a</sup>, Takashi Arii<sup>a</sup> and Yuki Shirosaki<sup>b</sup>  
8  
9

10  
11 <sup>a</sup>Graduate School of Life Science and System Engineering, Kyushu Institute of  
12 Technology, Kitakyushu, Japan  
13  
14

15  
16 <sup>b</sup>Faculty of Engineering, Kyushu Institute of Technology, Kitakyushu, Japan  
17  
18  
19  
20  
21

22 Corresponding author:  
23

24 Toshiki Miyazaki  
25

26  
27 Graduate School of Life Science and Systems Engineering, Kyushu Institute of  
28 Technology, 2-4, Hibikino, Wakamatsu-ku, Kitakyushu 808-0196, Japan  
29  
30

31 Tel/Fax: +81-93-695-6025  
32

33 E-mail: tmiya@life.kyutech.ac.jp  
34  
35  
36  
37  
38  
39  
40  
41  
42  
43  
44  
45  
46  
47  
48  
49  
50  
51  
52  
53  
54  
55  
56  
57  
58  
59  
60  
61  
62  
63  
64  
65

1  
2  
3 **Abstract**  
4  
5  
6

7 Calcium carbonate ( $\text{CaCO}_3$ ) can show various properties related to its different  
8  
9  
10 crystalline phases and is therefore a useful material for various applications. Wet  
11  
12  
13 processes are known to be suitable for preparing metastable  $\text{CaCO}_3$  polymorphs.  
14  
15  
16 Electrolysis has been proposed as a preparation method at ambient conditions. Although  
17  
18  
19 several electrolytic approaches have been reported, the effects of the applied current and  
20  
21  
22 temperature of the electrolyte on the crystalline phase and morphology of  $\text{CaCO}_3$  remain  
23  
24  
25 unclear. In the present study, we attempted the electrochemical preparation of  $\text{CaCO}_3$   
26  
27  
28 particles under various electrolysis conditions and discuss the mechanism of  $\text{CaCO}_3$   
29  
30  
31 particle formation. The crystalline phases and morphologies of the  $\text{CaCO}_3$  precipitates  
32  
33  
34 markedly changed depending on the applied current and method of cooling the  
35  
36  
37 electrolyte. We assume that these factors were governed by the degree of change in  
38  
39  
40 temperature, supersaturation, and pH of the electrolyte that were induced by differences  
41  
42  
43 in the electrolysis current.  
44  
45  
46  
47  
48  
49  
50

51 **Keywords:** A: Powders: chemical preparation, E: Biomedical applications,  $\text{CaCO}_3$   
52  
53  
54  
55  
56  
57  
58  
59  
60  
61

1  
2  
3 **Introduction**  
4  
5  
6

7 Calcium carbonate ( $\text{CaCO}_3$ ), an inorganic substance composed of common elements,  
8  
9  
10 has attracted considerable attention as a material with a low environmental burden and  
11  
12  
13 low risk of resource depletion.  $\text{CaCO}_3$  exhibits various properties that depend on its  
14  
15  
16 crystalline phase; for example, the aragonite phase has excellent mechanical strength  
17  
18  
19 owing to its high density [1], whereas the vaterite phase has high water solubility [2]. In  
20  
21  
22 the field of biomaterials, vaterite has attracted attention as a novel bioresorbable  
23  
24  
25 material with high biological affinity. A nonwoven fabric for bone repair has been  
26  
27  
28 prepared from vaterite and poly-L-lactic acid by electrospinning [3] and bioresorbable  
29  
30  
31 vaterite microspheres combined with silicate have been developed for bone-forming  
32  
33  
34 applications [4].  
35  
36  
37  
38  
39  
40  
41

42 Wet processes are suitable for preparing  $\text{CaCO}_3$  with a metastable phase. Crystalline  
43  
44  
45 phase control has been attempted by addition of organic substances in aqueous  
46  
47  
48 precipitation processes [5,6]. Furthermore, electrolysis has been proposed as a method  
49  
50  
51 to prepare  $\text{CaCO}_3$  polymorphs at ambient conditions. Watanabe et al. applied an  
52  
53  
54 alternating current of 10 V/cm to a glass cell containing calcium chloride and sodium  
55  
56  
57  
58  
59  
60  
61  
62  
63  
64  
65

1  
2  
3 carbonate solutions separated by a membrane and obtained a mixture of calcite and  
4  
5  
6  
7 vaterite with a small amount of aragonite [7]. Yamada et al. applied a direct current of 3  
8  
9  
10 to 10 V to a cell containing calcium nitrate and sodium hydrogen carbonate (NaHCO<sub>3</sub>)  
11  
12  
13 solutions separated by a membrane. In this case, addition of sodium nitrate to the  
14  
15  
16  
17 electrolyte effectively enhanced the formation of both calcite and vaterite [8]. The  
18  
19  
20 effects of the electrolysis conditions on the crystalline phase and morphology of CaCO<sub>3</sub>  
21  
22  
23  
24 nevertheless remain unclear.  
25  
26

27  
28 In the present study, we attempted to prepare CaCO<sub>3</sub> particles by an electrochemical  
29  
30  
31 method by varying the direct electric current and temperature. We discuss the  
32  
33  
34  
35 mechanism of CaCO<sub>3</sub> formation in detail.  
36  
37  
38  
39  
40  
41

## 42 **Materials and Methods**

43  
44  
45 Calcium nitrate tetrahydrate [Ca(NO<sub>3</sub>)<sub>2</sub>·4H<sub>2</sub>O] and hydrochloric acid (HCl) were  
46  
47  
48 purchased from Wako Pure Chemical Co., Japan. NaHCO<sub>3</sub> and  
49  
50  
51 tris(hydroxymethyl)aminomethane (Tris) were purchased from Nacalai Tesque Inc.,  
52  
53  
54  
55  
56 Japan. The electrolytic cell is shown in Figure 1. The anode and cathode chambers were  
57  
58  
59  
60  
61

1  
2  
3 filled with 100 mL of 0.5 M  $\text{Ca}(\text{NO}_3)_2$  aqueous solution and an equal volume of 0.5 M  
4  
5  
6  
7  $\text{NaHCO}_3$  aqueous solution, respectively. Both solutions were buffered at pH 8.5 by Tris  
8  
9  
10 and HCl. The reaction compartment between the chambers was filled with 220 mL of  
11  
12  
13 Tris buffer at pH 8.5. Platinum foils (Nilaco Co., Japan), 50 mm  $\times$  10 mm  $\times$  0.1 mm in  
14  
15  
16 size, were used for the electrodes. Constant direct current (DC) ranging from 0.2 to 0.6  
17  
18  
19 A was applied by a power supply (ZX-400M, Takasago Ltd., Japan) to the cell for  
20  
21  
22 various periods up to 30 min. At some conditions, the temperature of the electrolyte in  
23  
24  
25 the cell was controlled by use of cooling water and ice. Precipitates that formed in the  
26  
27  
28 reaction chamber were collected by vacuum filtration and dried at 60 °C.  
29  
30  
31  
32  
33

34  
35 The microstructure of the precipitates was analyzed by powder X-ray diffraction  
36  
37  
38 (XRD; MXP3V, Mac Science Co., Japan) with a  $\text{CuK}\alpha$  X-ray source operating at 40 kV  
39  
40  
41 and 30 mA. We also performed scanning electron microscope (SEM; S-3500N, Hitachi  
42  
43  
44 Co., Japan) and transmission electron microscope (TEM; H-9000NAR, Hitachi Co.,  
45  
46  
47 Japan) imaging studies. For SEM observations, the sample surface was coated with  
48  
49  
50 Au–Pd alloy by ion sputtering (E-101, Hitachi Co., Japan). A focused ion beam (FIB,  
51  
52  
53 FB-2000A, Hitachi Co., Japan) was used to prepare thin films for TEM observations.  
54  
55  
56  
57  
58  
59  
60  
61  
62  
63  
64  
65

1  
2  
3  
4  
5  
6  
7 **Results**  
8

9  
10 For all conditions, white precipitates were observed in the reaction chamber about 2  
11 min after applying the DC electric field. XRD patterns of precipitates obtained at  
12  
13 various currents without temperature control or with ice cooling are shown in Figure 2.  
14  
15  
16  
17  
18  
19  
20  
21 At 0.2 and 0.4 A without temperature control, calcite, vaterite, and a small amount of  
22  
23 aragonite were formed; the amount of calcite was greater than that of the other phases.  
24  
25  
26  
27  
28 Conversely, vaterite was the main crystalline phase and a small amount of calcite was  
29  
30 formed at 0.4 A with ice cooling. In addition, the amount of aragonite formed at 0.6 A  
31  
32 was much greater than in any of the other samples.  
33  
34  
35  
36

37  
38  
39 SEM images of the precipitates obtained at various currents without temperature  
40  
41 control or with ice cooling are shown in Figure 3. The morphologies of the precipitates  
42  
43 changed markedly depending on the current value and cooling method, as summarized  
44  
45  
46  
47  
48  
49 in Table 1. The shapes of the particles, as shown in Table 1, are schematically illustrated  
50  
51  
52  
53 in Fig. 4.

54  
55  
56 The temperature increased as the current was increased (Figure 5). Even with  
57  
58  
59  
60  
61



1  
2  
3 ice cooling, at 0.4 A, the temperature increased to 45 °C within 30 min. We assume that  
4  
5  
6  
7 the heat generated by the electrolyte at 0.4 A was too high to be maintained at a constant  
8  
9  
10 temperature by the ice bath.  
11

12  
13 Figure 6 shows XRD patterns of precipitates obtained at constant temperature and 0.2  
14  
15  
16  
17 A. The peak intensity of the vaterite increased as the temperature increased and the  
18  
19  
20 amount of calcite formed was slightly higher at 30 °C than at other temperatures.  
21  
22  
23

24 Figure 7 shows SEM images of precipitates obtained at constant temperature and 0.2  
25  
26  
27  
28 A. The morphology of the vaterite particles changed from spherical to  
29  
30  
31 hexagonal-shaped, and finally to flower-like, as the temperature was increased (Table  
32  
33  
34  
35 1).  
36  
37

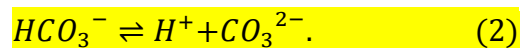
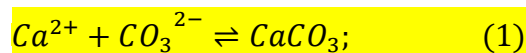
38 SEM images of the spherical particles prepared at 0.2 A and 25 °C are shown in  
39  
40  
41  
42 Figure 8 at low and high magnification. Spherical vateriate was covered with many  
43  
44  
45 nanoparticles, of 50 to 100 nm in size.  
46  
47

48 TEM images and electron diffraction patterns of the surface and inside of particles  
49  
50  
51 prepared at 0.4 A with ice cooling are shown in Figure 9. Diffraction rings and  
52  
53  
54  
55  
56 diffraction spots from the (200) spacing of vaterite were observed on the surface and  
57  
58  
59  
60  
61

1  
2  
3 inside of the particles, respectively; thus, the surface and inside of the hexagonal  
4  
5  
6  
7 particles comprised vaterite polycrystals and single crystals with c-axis orientation,  
8  
9  
10 respectively.  
11

## 12 13 14 15 16 17 **Discussion** 18

19  
20  $\text{CaCO}_3$  was precipitated by simple electrolysis reactions.  $\text{Ca}^{2+}$  diffuses from the  
21  
22  
23  
24 anode to the cathode under a DC electric field, while  $\text{CO}_3^{2-}$  diffuses in the reverse  
25  
26  
27  
28 direction. Limiting ionic conductance of  $\text{Ca}^{2+}$  ( $119.0 \text{ S}\cdot\text{cm}^2/\text{mol}$ ) is relatively close to  
29  
30  
31 that of  $\text{CO}_3^{2-}$  ( $138.6 \text{ S}\cdot\text{cm}^2/\text{mol}$ ) [9], which means that their ionic mobilities are also  
32  
33  
34  
35 similar; therefore, precipitation of  $\text{CaCO}_3$  would not occur in the anode or cathode  
36  
37  
38  
39 chamber, but in the reaction chamber. It is known that about 95 mol% of carbonate ion  
40  
41  
42 exists in the form of  $\text{HCO}_3^-$  at pH 8.5 [10].  $\text{CaCO}_3$  with low water solubility is formed  
43  
44  
45 by Equation (1) to consume  $\text{CO}_3^{2-}$ ; therefore, the equilibrium in Equation (2) is shifted  
46  
47  
48  
49 to the right:  
50



1  
2  
3 We found that the crystalline phase of electrochemically produced  $\text{CaCO}_3$  can be  
4  
5  
6 controlled by the applied current. The aragonite phase, which is normally difficult to  
7  
8  
9 obtain by electrolytic methods, was obtained by increasing the current. Generally,  
10  
11  
12 aragonite can be prepared in solutions at high temperatures [11]; therefore, increasing  
13  
14  
15 the electrolyte temperature at high current promoted aragonite formation. Monolithic  
16  
17  
18 aragonite was not obtained in the present study. Wang et al. demonstrated that  
19  
20  
21 monolithic aragonite is difficult to obtain without stirring of the solution, even at high  
22  
23  
24 temperature [12]. Monolithic samples are preferable for many practical applications;  
25  
26  
27 therefore, the addition of flow apparatus to our reaction chamber or addition of an  
28  
29  
30 aragonite stabilizer, such as  $\text{Mg}^{2+}$ , might be applied to our system to achieve such  
31  
32  
33 morphology.  
34  
35  
36  
37  
38  
39  
40  
41

42 The crystalline phases and morphologies of the precipitates was markedly affected by  
43  
44  
45 the method of temperature control, even at the same current (see Figs. 2 and 3), i.e.,  
46  
47  
48 particles with a hexagonal shape formed at 0.4 A with ice cooling, whereas many  
49  
50  
51 flower-like particles formed under all current conditions without temperature control.  
52  
53  
54

55  
56 Kojima et al. prepared  $\text{CaCO}_3$  particles with different crystalline phases and  
57  
58  
59  
60  
61  
62  
63  
64  
65

1  
2  
3 morphologies by heating of  $\text{Ca}(\text{HCO}_3)_2$  solutions at different temperatures and pH, and  
4  
5  
6  
7 precisely investigated the mechanism of  $\text{CaCO}_3$  formation [13]. They showed that the  
8  
9  
10 morphology of the vaterite changed from hexagonal to flower-like as the pH decreased.  
11  
12  
13 In the present study, the pH of the electrolyte tended to decrease when temperature was  
14  
15  
16 uncontrolled (i.e., pH 8.4 at 0.2 A and 30 °C after 30 min, compared with pH 7.9 at 0.2  
17  
18  
19 A without temperature control), in agreement with the above study. Therefore,  
20  
21  
22 decreasing pH promotes the formation of flower-like particles.  
23  
24  
25  
26  
27

28 When the temperature of the electrolyte was maintained constant, the morphology of  
29  
30  
31 the vaterite changed from hexagonal to flower-like as the temperature was increased  
32  
33  
34 (see Fig. 7). The solubility of  $\text{CaCO}_3$  decreases as temperature increases [14]; therefore,  
35  
36  
37  
38 an increase in the degree of supersaturation with respect to  $\text{CaCO}_3$  at high temperature  
39  
40  
41 promoted the formation of flower-like particles. We note that the morphology of the  
42  
43  
44 present particles was governed not only by pH, but also by the degree of  
45  
46  
47 supersaturation.  
48  
49  
50  
51

52 A greater amount of calcite was formed without temperature control than with ice  
53  
54  
55 cooling, even at the same current of 0.4 A (see Fig. 2). When the temperature was set to  
56  
57  
58  
59  
60  
61  
62  
63  
64  
65

1  
2  
3 0.2 A, the amount of calcite was slightly greater at 30 °C than at other temperatures (see  
4  
5  
6  
7 Fig. 6). Kojima et al. demonstrated that a single phase of calcite was formed at 30 °C  
8  
9  
10 [13]; therefore, we assume that the electrolyte temperature was maintained at  
11  
12  
13 approximately 30 °C for a longer time for the former than the latter, giving rise to a  
14  
15  
16  
17 greater amount of calcite.  
18  
19  
20

21 Spherical and hexagonal vaterite were observed at low and high temperatures,  
22  
23  
24 respectively (see Figs. 8 and 9). Their formation mechanism is schematically illustrated  
25  
26  
27 in Fig. 10. At low temperatures, small nuclei formed: their growth was suppressed  
28  
29  
30 owing to the low degree of supersaturation, but nucleation was enhanced by ion  
31  
32  
33 diffusion from the anodic and cathodic chambers and the subsequent increase in the  
34  
35  
36 degree of supersaturation. Small crystallites aggregated to form spherical particles, as  
37  
38  
39 shown in Fig. 8. Conversely, at high temperatures, the formed nuclei vigorously grew  
40  
41  
42 into hexagonal particles, owing to the degree of high supersaturation, and then  
43  
44  
45  
46 secondary nucleation occurred by ion diffusion from the chambers.  
47  
48  
49  
50

51  
52  
53 Vaterite single crystals with a similar morphology to that of our particles in Fig. 9  
54  
55  
56 were reported by Zhan et al. [15]. They investigated the formation process of vaterite  
57  
58  
59  
60  
61  
62  
63  
64  
65

1  
2  
3 prepared by heating of an aqueous mixture of calcium nitrate, gelatin, and urea at  
4  
5  
6  
7 100 °C. Hexagonal crystals covered with nanoparticles formed at 6 h, which  
8  
9  
10 transformed to single crystals with clear facets after 1 day. They speculated that the high  
11  
12  
13 concentration of gelatin (10 mass%) played an important role in oriented aggregation  
14  
15  
16 growth. In the present study, the organic Tris concentration in the electrolyte was only  
17  
18  
19  
20  
21 50 mM; therefore, it would have a small influence on the crystal growth. The formation  
22  
23  
24 of CaCO<sub>3</sub> mesocrystals in a DC electric field has also been reported [16]; therefore,  
25  
26  
27 oriented aggregation growth of vaterite in the present study would be induced by the  
28  
29  
30  
31 applied electric field.  
32  
33

34  
35 We expect that vaterite particles with different morphologies will have applications as  
36  
37  
38 bioresorbable drug delivery carriers with desirable release profiles, because the surface  
39  
40  
41 area differs between single crystals and polycrystals.  
42  
43  
44  
45  
46  
47  
48

## 49 **Conclusions**

50  
51  
52 It was found that CaCO<sub>3</sub> particles with different crystalline phases and morphologies  
53  
54  
55  
56 can be electrochemically fabricated by changing the applied direct current and  
57  
58  
59  
60  
61  
62  
63  
64  
65

1  
2  
3 electrolyte temperature. In particular, the aragonite phase, which is normally difficult to  
4  
5  
6  
7 obtain by electrolytic methods, was observed at high current. Knowledge from the  
8  
9  
10 present study can provide a fundamental approach to designing CaCO<sub>3</sub> with desired  
11  
12  
13 mechanical and biological properties by electrochemical processing.  
14  
15  
16  
17  
18  
19  
20

## 21 **Acknowledgment**

22  
23  
24 We thank Andrew Jackson, PhD, and Kathryn Sole, PhD, from Edanz Group  
25  
26  
27  
28 (www.edanzediting.com/ac) for editing drafts of this manuscript.  
29  
30  
31  
32  
33  
34

## 35 **References**

- 36  
37  
38  
39 1. J. Sun, B. Bhushan, Hierarchical structure and mechanical properties of nacre: a  
40  
41  
42 review, RSC Adv. 2 (2012) 7617-7632. <https://doi.org/10.1039/C2RA20218B>  
43  
44  
45  
46 2. L.N. Plummer, E. Busenberg, The solubilities of calcite, aragonite and vaterite in  
47  
48  
49 CO<sub>2</sub>-H<sub>2</sub>O solutions between 0 and 90°C, Geochim. Cosmochim. Acta, 46 (1982)  
50  
51  
52 1011-1040. [https://doi.org/10.1016/0016-7037\(82\)90056-4](https://doi.org/10.1016/0016-7037(82)90056-4)  
53  
54  
55  
56 3. A. Obata, T. Hotta, T. Wakita, Y. Ota, T. Kasuga, Electrospun microfiber meshes of  
57  
58  
59  
60  
61  
62  
63  
64  
65

- 1  
2  
3 silicon-doped vaterite/poly (lactic acid) hybrid for guided bone regeneration, *Acta*  
4  
5  
6  
7 *Biomater.* 6 (2010) 1248-1257. <https://doi.org/10.1016/j.actbio.2009.11.013>  
8  
9
- 10 4. J. Nakamura, G. Poologasundarampillai, J.R. Jones, T. Kasuga, Tracking the  
11  
12 formation of vaterite particles containing aminopropyl-functionalized  
13  
14 silsesquioxane and their structure for bone regenerative medicine, *J. Mater. Chem.*  
15  
16  
17  
18 *B* 1 (2013) 4446-4454. <https://doi.org/10.1039/C3TB20589D>  
19  
20  
21  
22
- 23 5. N. Hosoda, T. Kato, Thin-film formation of calcium carbonate crystals: effects of  
24  
25 functional groups of matrix polymers, *Chem. Mater.* 13 (2001) 688-693.  
26  
27  
28  
29  
30  
31  
32 <https://doi.org/10.1021/cm000817r>  
33  
34
- 35 6. Y. Zhao, Z. Chen, H. Wang, J. Wang, Crystallization control of CaCO<sub>3</sub> by ionic  
36  
37  
38 liquids in aqueous solution, *Cryst Growth Des.* 9 (2009) 4984-4986.  
39  
40  
41  
42  
43 <https://doi.org/10.1021/cg900771c>  
44  
45
- 46 7. J. Watanabe, M. Akashi, Formation of various polymorphs of calcium carbonate on  
47  
48  
49 porous membrane by electrochemical approach, *J. Cryst. Growth* 311 (2009)  
50  
51  
52  
53 3697-3701. <https://doi.org/10.1016/j.jcrysgr.2009.06.016>  
54  
55
- 56 8. K. Yamada, M. Ohta, K. Hirano, T. Kimura, Preparation of calcium carbonate in an  
57  
58  
59  
60  
61  
62  
63  
64  
65



1  
2  
3 electrolytic cell, *Inorg. Mater.*, 4 (1997) 609-612 (in Japanese).  
4  
5

6  
7 9. J.A. Dean, *Lange's Handbook of Chemistry*, fifteenth ed., McGraw-Hill, New York,  
8  
9 1999.  
10  
11

12  
13 10. K.M. Steel, K. Alizadehhesari, R.D. Balucan, B.Bašić, Conversion of CO<sub>2</sub> into  
14  
15 mineral carbonates using a regenerable buffer to control solution pH, *Fuel*, 111  
16  
17 (2013) 40-47. <https://doi.org/10.1016/j.fuel.2013.04.033>  
18  
19  
20  
21  
22

23  
24 11. Y. Ota, S. Inui, T. Iwashita, T. Kasuga, Y. Abe, Preparation conditions for aragonite  
25  
26 whiskers by carbonation process, *J. Ceram. Soc. Japan*, 104 (1996) 196-200 (in  
27  
28 Japanese). <https://doi.org/10.2109/jcersj.104.196>  
29  
30  
31

32  
33 12. H. Wang, W. Huang, Y. Han, Diffusion-reaction compromise the polymorphs of  
34  
35 precipitated calcium carbonate, *Particuology*, 11 (2013) 301-308.  
36  
37  
38  
39  
40  
41  
42 <https://doi.org/10.1016/j.partic.2012.10.003>  
43  
44

45  
46 13. Y. Kojima, A. Sadotomo, T. Yasue, Y. Arai, Control of crystal shape and  
47  
48 modification of calcium carbonate prepared by precipitation from calcium  
49  
50 hydrogencarbonate solution, *J. Ceram. Soc. Japan*, 100 (1992) 1145-1153 (in  
51  
52 Japanese). <https://doi.org/10.2109/jcersj.100.1145>  
53  
54  
55  
56  
57

- 1  
2  
3  
4 14. B. Coto, C. Martos, J.L. Peña, R. Rodríguez, G. Pastor, Effects in the solubility of  
5  
6  
7 CaCO<sub>3</sub>: experimental study and model description, Fluid Phase Equilibria, 324  
8  
9  
10 (2012) 1-7. <https://doi.org/10.1016/j.fluid.2012.03.020>  
11  
12  
13  
14 15. J. Zhan, H.P. Lin, C.Y. Mou, Biomimetic formation of porous single-crystalline  
15  
16  
17 CaCO<sub>3</sub> via nanocrystal aggregation, Adv. Mater., 15 (2003) 621-623.  
18  
19  
20  
21 <https://doi.org/10.1002/adma.200304600>  
22  
23  
24  
25 16. J. Qi, R. Guo, Y. Wang, X. Liu, H. Chan, Electric field-controlled crystallizing  
26  
27  
28 CaCO<sub>3</sub> nanostructures from solution, Nanoscale Res. Lett. 11 (2016) 120.  
29  
30  
31  
32 <https://doi.org/10.1186/s11671-016-1338-4>  
33  
34  
35  
36  
37  
38  
39  
40  
41  
42  
43  
44  
45  
46  
47  
48  
49  
50  
51  
52  
53  
54  
55  
56  
57  
58  
59  
60  
61  
62  
63  
64  
65

1  
2  
3 **Table caption**

4 **Table 1** Morphology of the precipitates prepared by various conditions  
5  
6

7  
8 **Figure captions**

9 **Figure 1** Appearance of electrolytic cell.  
10

11 **Figure 2** X-ray diffraction patterns of precipitates obtained at various currents without  
12 temperature control and with ice cooling.  
13

14 **Figure 3** Scanning electron micrograph of precipitates obtained at various currents  
15 without temperature control and with ice cooling.  
16

17 **Figure 4** Schematic illustration of shapes of precipitates formed under different  
18 electrolytic conditions.  
19

20 **Figure 5** Changes in temperature of the electrolyte.  
21

22 **Figure 6** X-ray diffraction patterns of precipitates obtained at various constant  
23 temperatures and 0.2 A.  
24

25 **Figure 7** Scanning electron micrographs of precipitates obtained at various constant  
26 temperatures and 0.2 A.  
27

28 **Figure 8** Scanning electron micrographs of spherical particles prepared at 0.2 A and  
29 25 °C at low and high magnifications.  
30

31 **Figure 9** Transmission electron micrographs and electron diffraction patterns of the  
32 surface and inside of particles prepared at 0.4 A with ice cooling.  
33

34 **Figure 10** Schematic illustration of the formation mechanism of vaterite particles with  
35 different morphologies.  
36  
37  
38  
39  
40  
41  
42  
43  
44  
45  
46  
47  
48  
49  
50  
51  
52  
53  
54  
55  
56  
57  
58  
59  
60  
61  
62  
63  
64  
65

Table 1 Morphology of the precipitates prepared by various conditions

Current / A	Temperature control	Morphology				
		Spherical	Rhombohedral	Hexagonal	Flower-like	Rod-like
0.2	No	Yes	Yes	No	Yes	No
0.4	No	Yes	Yes	No	Yes	Yes
0.4	Ice cooling	Yes	No	Yes	No	Yes
0.6	No	No	No	No	Yes	Yes

Figure1

[Click here to download high resolution image](#)

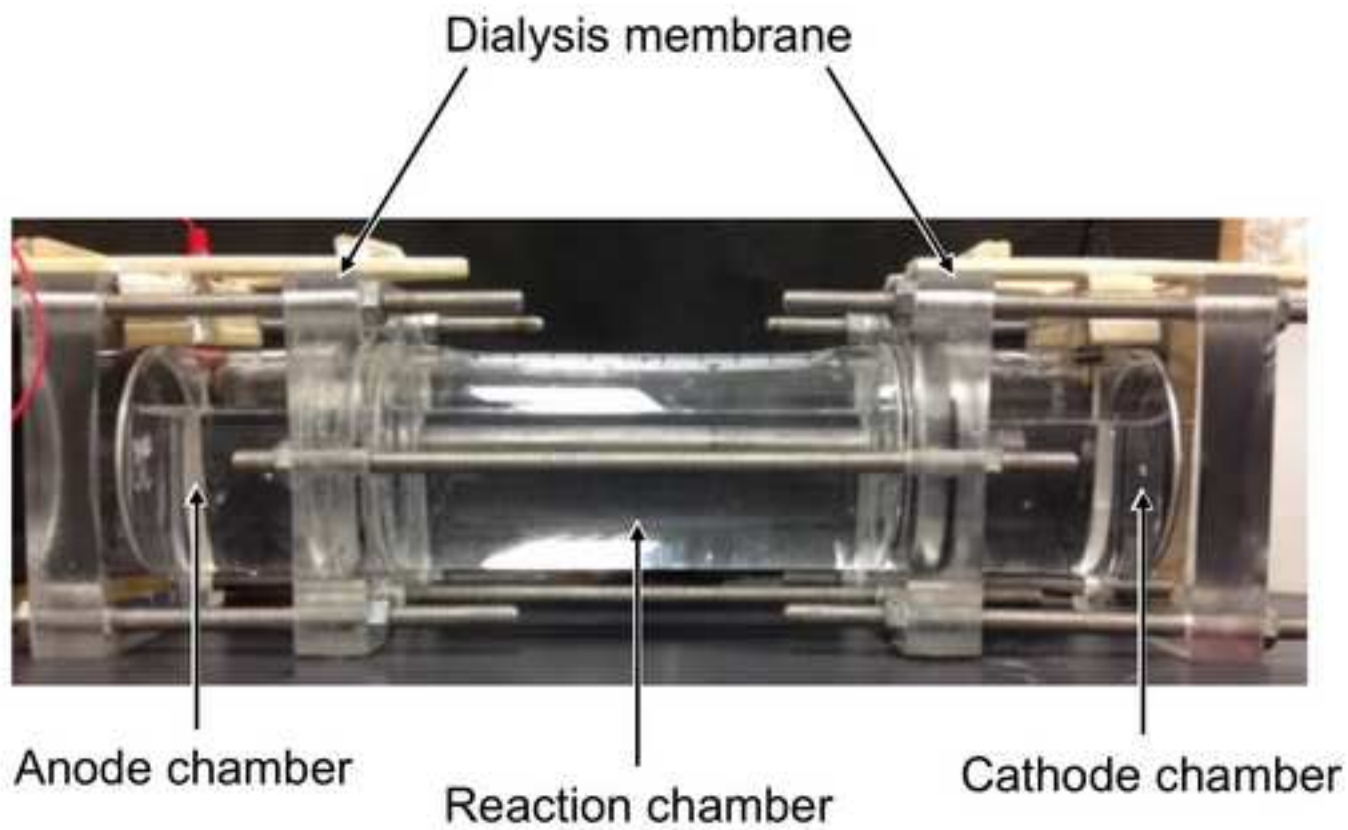


Fig. 1

Figure2

[Click here to download high resolution image](#)

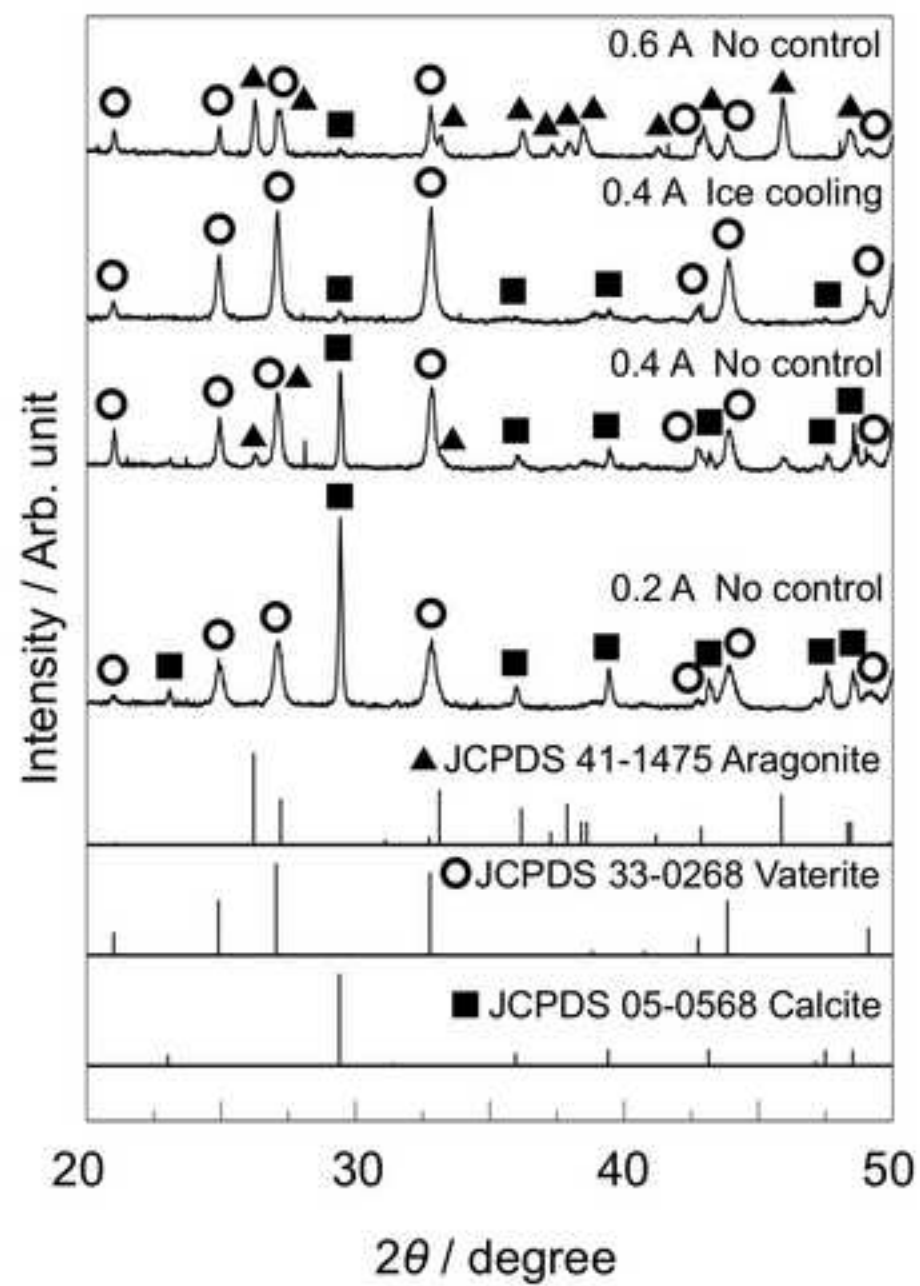


Fig. 2

Figure3

[Click here to download high resolution image](#)

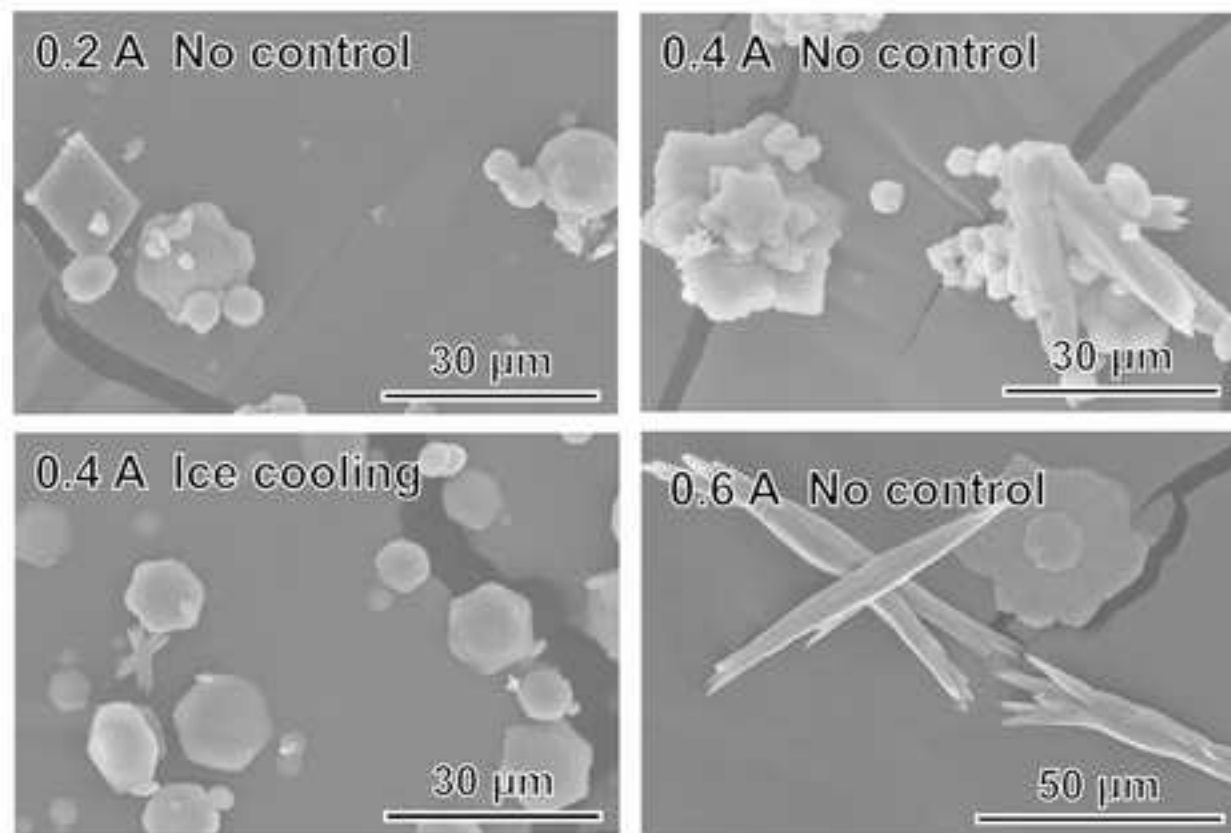
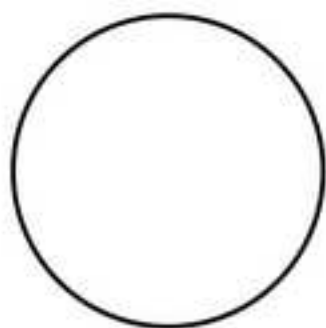


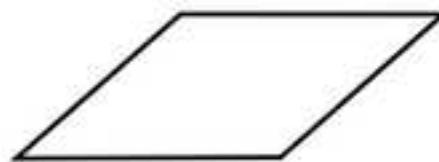
Fig. 3

Figure4

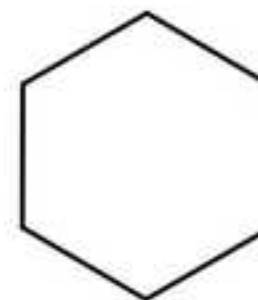
[Click here to download high resolution image](#)



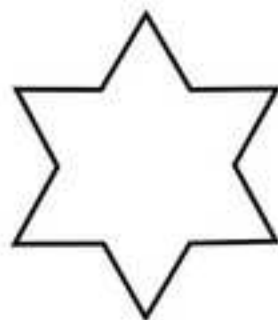
Spherical



Rhombohedral



Hexagonal



Flower-like



Rod-like

Fig. 4



Figure5

[Click here to download high resolution image](#)

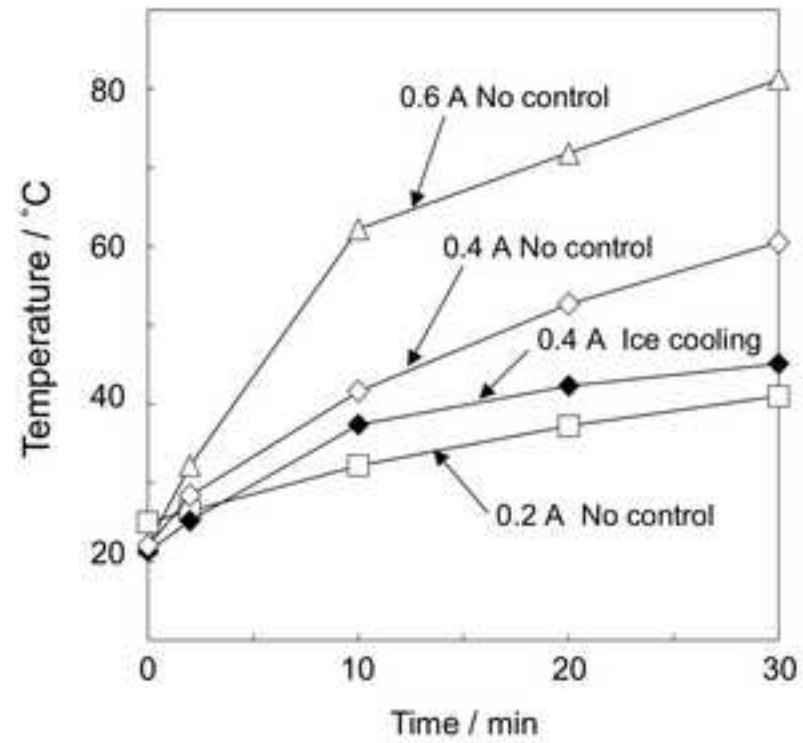


Fig. 5

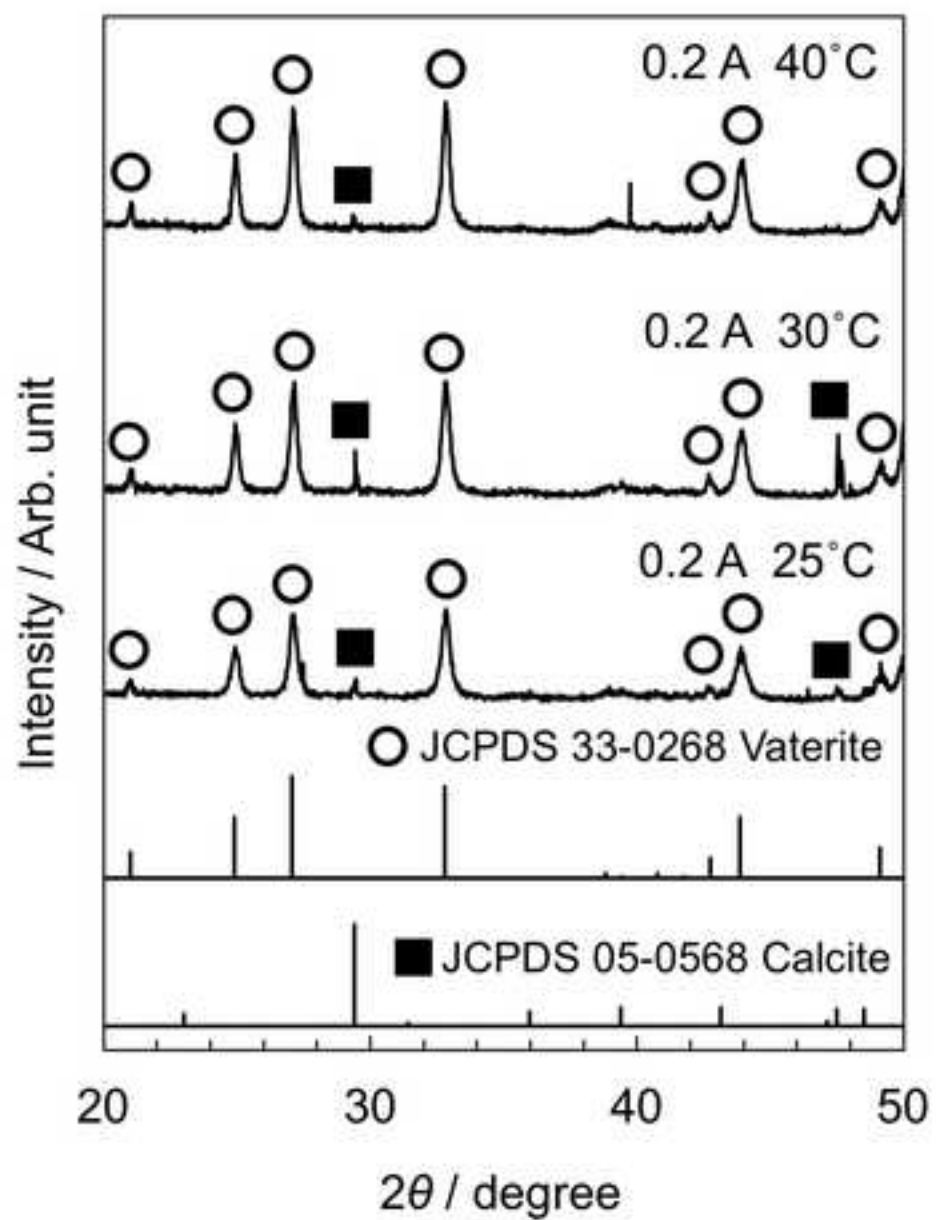


Fig. 6

Figure7

[Click here to download high resolution image](#)

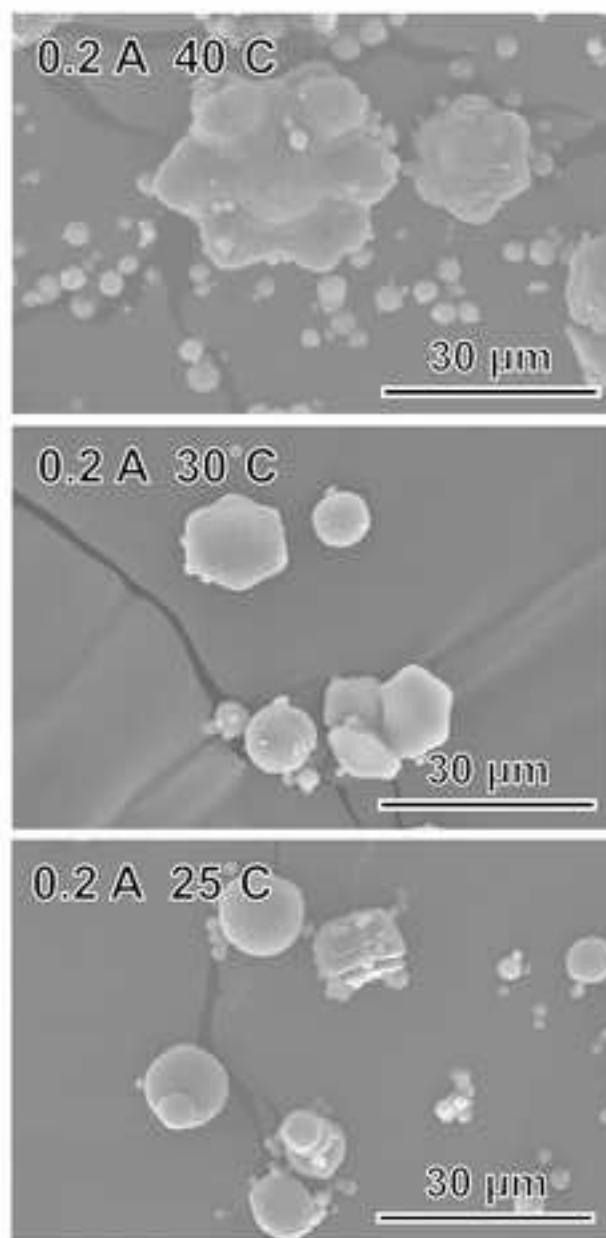


Fig. 7

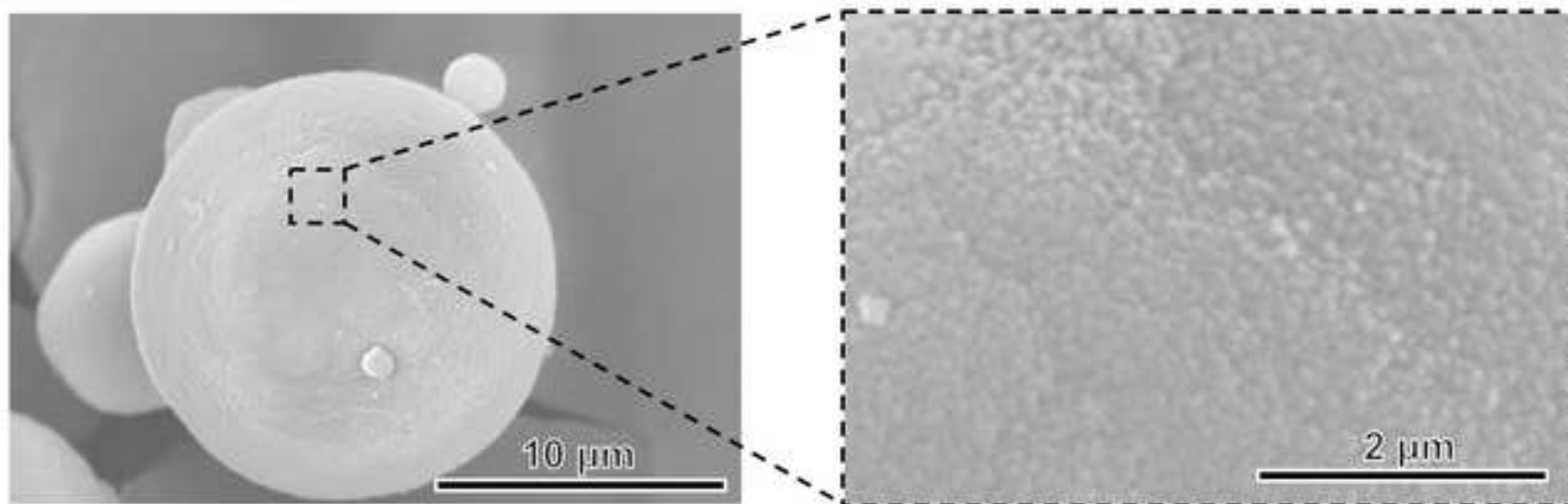
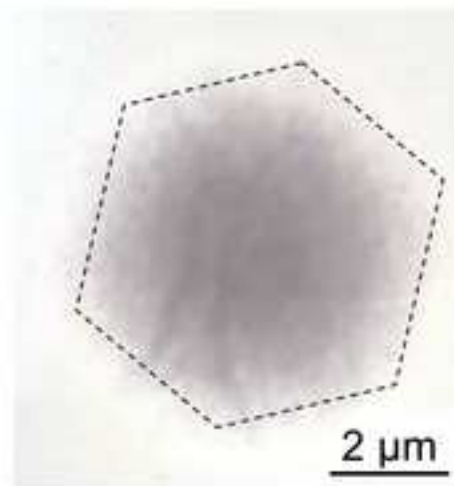


Fig. 8

Figure9

[Click here to download high resolution image](#)

Surface



Inside



Fig. 9

Low temperature

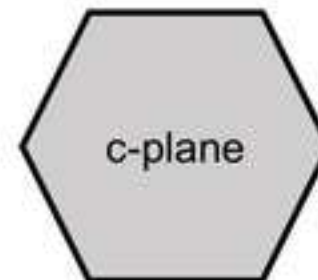


Formation of small single crystals due to low supersaturation degree



Suppression of growth of the single crystals to aggregate each other

High temperature



Vigorous growth of single crystals due to high supersaturation degree



Secondary nucleation around the grown single crystals

Initial stage

Later stage

Fig. 10